ELSEVIER

Nuclear Physics A575 (1994) 374–380

NUCLEAR PHYSICS A

Subbarrier fusion of $^{16}O + ^{112}Cd$: Cross sections and mean angular momenta ☆

D. Ackermann *, L. Corradi, D.R. Napoli, C.M. Petrache †, P. Spolaore, A.M. Stefanini

Istituto Nazionale di Fisica Nucleare, Laboratori Nazionali di Legnaro, I-35020 Legnaro (Padova), Italy

F. Scarlassara, S. Beghini, G. Montagnoli, G.F. Segato, C. Signorini

Dipartimento di Fisica, Università di Padova and Istituto Nazionale di Fisica Nucleare, Sezione di Padova, I-35100 Padova, Italy

Received 24 January 1994; revised 23 March 1994

Abstract

Fusion cross sections and mean angular momenta have been measured for $^{16}O + ^{112}Cd$ around the Coulomb barrier. The experimental results are well reproduced by coupled-channels calculations, confirming the validity of this model for mass-asymmetric systems. The predicted asymptotic behaviour of the mean angular momentum at low energies has been observed.

Key words: NUCLEAR REACTIONS $^{16}O + ^{112}Cd$; $E_{lab} = 52.2–69.1$ MeV; measured evaporation residues and coincident γ-rays; deduced excitation function $\sigma(E)$ and mean-spin distribution $\langle l \rangle(E)$ around, below the Coulomb barrier; coupled-channels calculations; enriched targets; electrostatic beam separator.

1. Introduction

In recent years the angular momentum of compound nuclei produced in heavy-ion collisions has been recognized to be an important parameter for the

* Corresponding author. Supported by a grant of the Commission of the European Communities.

† Corresponding author. On leave from the Institute of Physical and Nuclear Engineering, Bucarest, Romania.

☆ This work is part of the Ph.D. thesis of D. Ackermann.

Elsevier Science B.V.
SSDI 0375-9474(94)00177-O

understanding of nuclear reactions around the Coulomb barrier [1]. In particular the measurement of the mean angular momentum $\langle l \rangle$ provides, as a complementary tool to the fusion cross section σ_{fus}, additional information on the fusion process. A qualitative and to some extent also quantitative description of fusion has been achieved by coupled-channels (CC) models (see e.g. ref. [2]). A systematic comparison of data with CC calculations shows [3] that the model underpredicts both $\langle l \rangle$ and σ_{fus} at energies below the barrier for heavy and (quasi-)symmetric systems, whereas it works rather well for light and/or asymmetric ones. We reported before [4] on measurements of $\langle l \rangle$ and σ_{fus} for the rather symmetric systems ^{64}Ni + ^{92,96}Zr where a striking discrepancy between experiment and theory was found for both quantities.

Here we present the results of the measurement of fusion cross sections and mean angular momenta for the asymmetric reaction ^{16}O + ^{122}Cd in an energy interval from 52.2 MeV to 69.1 MeV in the laboratory system, ranging from below to well above the Coulomb barrier. In sect. 2 we restrict ourselfes to briefly describing the experimental setup and the data analysis. In sect. 3 the fusion-excitation function and the mean-spin distribution are compared with CC calculations. Sect. 4 gives a summary of this work.

2. Experiment and data analysis

The experiment was performed at the XTU Tandem accelerator facility of the Laboratori Nazionali di Legnaro, using ^{16}O beams with typical beam currents of ≈ 5 pnA. As targets we used sandwiches of 100 μg/cm^2 Au–150 μg/cm^2 ^{112}Cd–10 μg/cm^2 carbon and 80 μg/cm^2 ^{112}Cd–10 μg/cm^2 carbon. The cadmium was enriched to 97.05% in mass 112.

The setup consisted of an electrostatic beam deflector followed by a time-of-flight energy (t.o.f–E) telescope in combination with two 4″ × 4″ NaI(Tl) crystals placed at 90° to the beam line and at ≈ 10 cm from the target. For more information concerning technical details see refs. [4,5].

The evaporation residues (ER) were separated from the beamlike background in the two-dimensional plot t.o.f. versus E. Two angular distributions were measured at $E_{lab} = 61$ MeV and 55 MeV as shown in Fig. 1. Their width and shape do not vary with energy, as was expected in this case where neutron emission dominates the evaporation process. Therefore at all other energies where only 0° measurements were performed, an energy-independent factor was assumed to relate the 0° yields to the angle-integrated cross sections. The transmission of the electrostatic deflector was found to be (76 ± 11)%. The experimental errors due to the integration of the angular distributions, to the geometrical uncertainties and to the transmission (see refs. [4,5]) sum up to an estimated ± 20%. Statistical uncertainties are relevant only at the lowest measured energies. The obtained fusion-evaporation cross sections are listed in Table 1.

From the ratio of the ER with and without a coincidence condition with γ-rays detected in the NaI crystals, we deduced the average γ-multiplicities $\langle M_\gamma \rangle$ (see ref. [4]) listed in the table. The total γ-detection efficiency was around 5%. Following the considerations of ref. [4] the $\langle M_\gamma \rangle$ values were converted into $\langle l \rangle$ using the relation

$$\langle l \rangle = \Delta I_{ns}(\langle M_\gamma \rangle - M_{\gamma s}) + \sum_i \Delta I_i M_i + I_0, \quad \text{with } i = \gamma s, \text{n}, \text{p}, \alpha, \tag{1}$$

where ΔI_{ns} is the average spin removed by nonstatistical γ-rays, ΔI_i are the spins removed by statistical γ-rays (γs), neutrons (n), protons (p) and α-particles (α) and M_i are the corresponding multiplicities. I_0 denotes the ground-state spin of the ER.

At variance with the systems ^{64}Ni + ^{92,96}Zr no experimental values for ΔI_{ns} are known so that ΔI_{ns}, ΔI_i and M_i were all calculated with the evaporation code PACE2 [6] using standard parameters. The crucial factor in Eq. (1) is ΔI_{ns}. To estimate it, basic information on the evaporation process as ER probabilities, as well as their detailed nuclear structure, is needed. As in our case little experimental information on these properties is available, we relied on the model calculation, from which we obtain for ΔI_{ns} values slowly increasing from 1.5$\hbar$ to 1.8$\hbar$ in the measured energy range. This seems quite reasonable in comparison to what has been reported before [4,7]. Moreover, the increase of ΔI_{ns} with energy is consistent with the increase of the number of evaporated particles; in fact, the expected change of the main evaporation channel from the even–odd nucleus ^{123}Ba around and below the Coulomb barrier to the even–even nucleus ^{124}Ba at higher energies

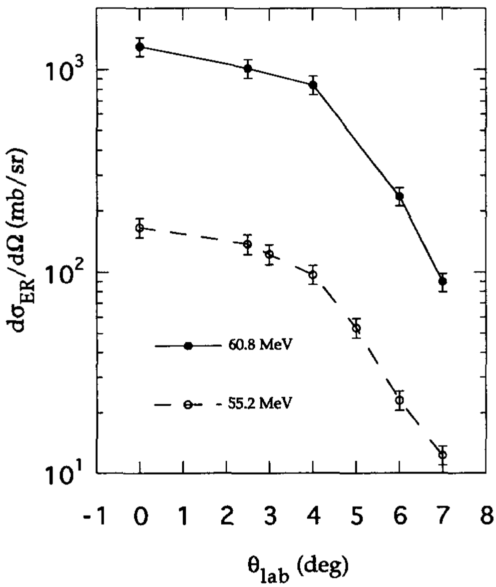

Fig. 1. Angular distributions of evaporation residues from the reaction ^{16}O + ^{112}Cd at the two indicated beam energies (the lines connecting the points are only visual guides).

Table 1
Experimental ER cross sections and mean angular momenta for the system $^{16}O+^{112}Cd$

$E_{c.m.}$ (MeV)	M_γ	$\langle l \rangle$ ($\hbar$)	σ_{ER} (mb)
45.3	3.8±0.6	6.3±1.1	1.8± 0.41
45.7	3.7±0.3	6.3±0.5	4.2± 0.86
46.6	4.0±0.6	6.8±1.0	9.4± 2.0
47.1	4.8±0.5	8.0±0.8	20.6± 4.1
47.8	4.8±0.3	8.2±0.6	48.0± 9.6
48.8	4.3±0.3	7.5±0.5	73.2± 14.7
49.6	5.3±0.3	9.2±0.6	124 ± 25
50.5	5.9±0.2	10.3±0.4	153 ± 31
51.4	6.7±0.4	11.8±0.8	206 ± 41
52.2	6.5±0.4	11.6±0.8	267 ± 54
52.7	7.0±0.4	12.5±0.8	385 ± 77
55.0	7.6±0.3	14.0±0.6	355 ± 71
56.6	8.4±0.4	15.9±0.7	628 ±126
60.1	9.3±0.5	18.8±1.0	853 ±171

should result in the observation of more γ-rays with multipolarity E2. The above mentioned ΔI_{ns} values correspond to E2/M1-ratios of 1 and 4 respectively.

The other parameters depend also on energy and we get $M_{\gamma s} = 2.0$–3.0, $\Delta I_{\gamma s} = (0.8$–$1.0)\hbar$, $M_n = 2.2$–2.5, $\Delta I_n = (0.2$–$0.9)\hbar$, $M_p = 0.4$–0.5, $\Delta I_p = (0.2$–$0.9)\hbar$, $M_\alpha = 0.0$–0.15 and $\Delta I_\alpha = (0.0$–$4.9)\hbar$. For each measured energy the corresponding calculated value of these parameters has been applied. The variation reflects the distribution of spin and excitation energy available for the various incident energies. However, the corrections for all these effects remain rather small, which is mainly due to the cited dominance of neutron evaporation. The ground-state spin was taken according to the relative production yield of the different ERs based also on PACE2 calculations and it depends on energy ($\Delta I_0 = (1.7$–$1.3)\hbar$). The deduced values for $\langle l \rangle$ are listed in the table. The errors are due to a 5% uncertainty in the NaI-detector efficiency plus the statistical ones.

3. Discussion of the results

The fusion-excitation function is shown in Fig. 2, where a comparison is done with simplified CC calculations performed with the CCfus code [8]. Here we included only the lowest quadrupole and octupole excitations of ^{112}Cd because of the rigid structure of ^{16}O. The coupling strengths were calculated with the deformation parameters β_λ taken from ref. [9] as $\beta_2 = 0.173$ (2^+; 617 keV) and $\beta_3 = 0.164$ (3^-; 2005 keV). We used the same potential as in ref. [4] varying only the radius parameter r_0 until the high-energy part of the measured excitation function was reproduced ($r_0 = 1.22$ fm; $V_0 = -58$ MeV; $a_0 = 0.63$ fm). Already the no-coupling calculation (tunneling through a one-dimensional barrier; dashed line) is close to the data points. The effect of the couplings is small and succeeds very well in reproducing the experiment.

In the coupled-channels approach of Dasso and Landowne [10] the relationship between fusion cross section and compound nucleus spin is given by

$$\sigma_l(E) = \frac{\hbar^2\pi}{2\mu E}\sum_i p_i(2l+1)$$
$$\times\left[1+\exp\left(\left(V_b + \frac{l(l+1)\hbar^2}{2\mu R_b^2} + \lambda_i - E\right)/\epsilon\right)\right]^{-1}, \qquad (2)$$

where ϵ is the curvature of the potential in the Hill–Wheeler approximation, p_i and λ_i are relative flux and barrier shift for the ith channel. Using such an ansatz the spin distribution shows the following dependence on energy [10]: above the Coulomb barrier $\sigma(l)$ has a triangular shape and $\langle l\rangle$ can be approximated by

$$\langle l\rangle = \tfrac{2}{3}\sqrt{2\mu R_b^2(E-V_b)\hbar^2}, \qquad (3)$$

varying quickly with energy. For energies much below the barrier the shape of the spin distribution becomes gaussian and does not change with energy. The mean angular momentum approaches a constant value

$$\langle l\rangle = \tfrac{4}{3}\sqrt{\mu R_b^2\epsilon/\hbar^2}. \qquad (4)$$

For strong coupling to nuclear-shape degrees of freedom or to other reaction channels a bump appears in the barrier region. This has been observed e.g. in the reaction $^{28}Si + ^{154}Sm$ [11], where the strong deformation of ^{154}Sm produces an ensemble of barriers according to the orientation of the symmetry axis with respect to the beam direction.

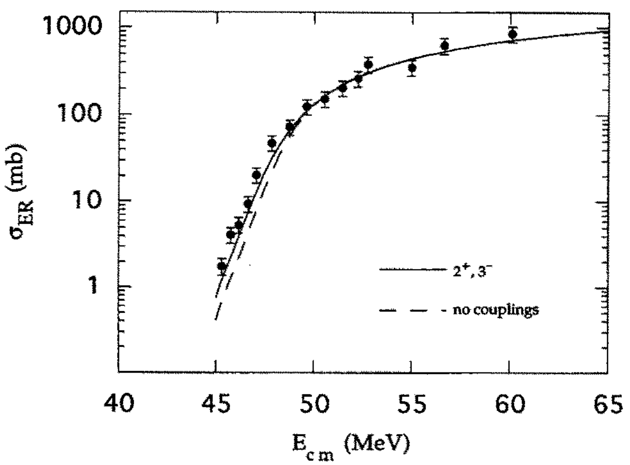

Fig. 2. Fusion-evaporation excitation function for the reaction $^{16}O + ^{112}Cd$. The data are compared with the results of CC calculations including the lowest 2^+ and 3^- target excitations (see text), and with the no-coupling limit (dashed line).

In Fig. 3 we compare our data on $\langle l \rangle$ with CC calculations (CCfus) using the same potential which reproduces the fusion-excitation function. As the coupling is weak, also the observed effect is small. The overall consistency between data and model predictions is very good and in particular the asymptotic constant behaviour in the low-energy domain is sufficiently clear. This feature was first observed using the isomer-ratio method [12] for several reactions leading to ^{137}Ce.

The direct relation between the fusion-excitation function $\sigma_{\mathrm{fus}}(E)$ and the single partial-wave cross sections σ_l has been pointed out first in ref. [13]. Assuming for the fusion probability $p(E, l)$

$$p(E, l) = p(E - E_{\mathrm{rot}}, l = 0), \tag{5}$$

i.e. the probability for s-wave fusion at a kinetic energy lowered by the centrifugal barrier $E_{\mathrm{rot}} = l(l+1)\hbar^2/2\mu R_{\mathrm{b}}^2$, one derives

$$p(E, l) = \frac{1}{\pi R_{\mathrm{b}}^2}\left(\left.\frac{\mathrm{d}(\sigma_{\mathrm{fus}})}{\mathrm{d}E}\right|_{(E-E_{\mathrm{rot}})} + \sigma_{\mathrm{fus}}(E - E_{\mathrm{rot}})\right). \tag{6}$$

Therefore, by fitting an analytic function to the measured fusion cross section [14] one obtains directly $\sigma_l(E)$ and $\langle l \rangle(E)$. The full curve in Fig. 3 has been obtained by this procedure and shows a very good agreement with both the $\langle l \rangle$ data and the CC-model predictions. In particular also the asymptotic behaviour in the low-energy region is reproduced.

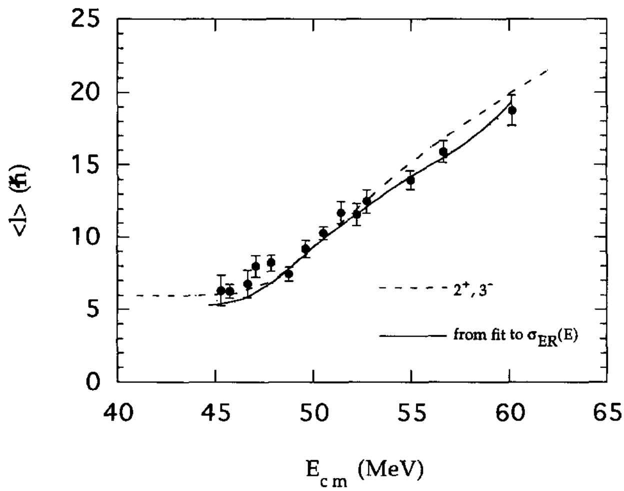

Fig. 3. Mean angular momenta for the fusion of ^{16}O + ^{112}Cd. The data are compared with the results of CC calculations including the lowest 2^+ and 3^- target excitations (dashed line), and with a curve obtained from a fit to the fusion-excitation function (see text; full line).

4. Summary

The results of σ_{fus} and $\langle l \rangle$ measurements for the system $^{16}O + ^{112}Cd$ have been presented. In contrast to the observations done in heavier ($M_{CN} \approx 150$) and more symmetric systems the predictions of simple CC calculations for the fusion process in the barrier and subbarrier region show a good overall agreement with the measured fusion cross sections and mean angular momenta. In particular the constant behaviour of $\langle l \rangle$ far below the barrier is evident. A good overall consistency with the data and the CC model shows up when applying an analytic procedure for the construction of $\langle l \rangle(E)$ directly from the measured fusion excitation function.

References

[1] R. Vandenbosch, Ann. Rev. Nucl. Part. Sci. 42 (1992) 447
[2] S. Landowne, Proc. Symp. on heavy ion interactions around the Coulomb barrier, Legnaro, Italy, 1988, eds. C. Signorini, S. Skorka, P. Spolaore and A. Vitturi (Springer, Berlin, 1988) p. 3
[3] D.E. DiGregorio and R.G. Stokstad, Phys. Rev. C43 (1991) 265
[4] A.M. Stefanini, L. Corradi, D. Ackermann, A. Facco, F. Gramegna, H. Moreno, L. Müller, D.R. Napoli, G.F. Prete, P. Spolaore, S. Beghini, D. Fabris, G. Montagnoli, G. Nebbia, J.A. Ruiz, G.F. Segato, C. Signorini and G. Viesti, Nucl. Phys. A548 (1992) 453
[5] S. Beghini, C. Signorini, S. Lunardi, M. Morando, G. Fortuna, A.M. Stefanini, W. Meczynski and R. Pengo, Nucl. Instr. Meth. A239 (1985) 585
[6] A. Gavron, Phys. Rev. C20 (1980) 230
[7] R.D. Fischer, A. Ruckelshausen, G. Koch, W. Kuehn, V. Metag, R. Muehlhans, R. Novotny, H. Stroeher, H. Groeger, D. Habs, H.W. Heyng, R. Pepnow, D. Schwalm, W. Reisdorf and R.S. Simon, Phys. Lett. B171 (1986) 33;
A. Ruckelshausen, B. Haas, D. Habs, R.V.F. Janssens, T.L. Khoo, W. Kuehn, V. Metag, D. Schwalm and R.S. Simon, Phys. Rev. Lett. 58 (1987) 1584
[8] C.H. Dasso and S. Landowne, Comput. Phys. Commun. 46 (1987) 187
[9] D. De Frenne, E. Jacobs and M. Verboven, Nucl. Data Sheets 57 (1989) 443
[10] C.H. Dasso and S. Landowne, Phys. Rev. C32 (1985) 1094
[11] S. Gil, D. Abriola, D.E. DiGregorio, M. di Tada, M. Elgue, M.C. Etchegoyen, J. Fernández Niello, A.M.J. Ferrero, A.O. Macchiavelli, A.J. Pacheco, J.E. Testoni, P. Silveira Gomes, V.R. Vanin, A. Charlop, A. García, S. Kailas, S.J. Luke, E. Renshaw and R. Vandenbosch, Phys. Rev. Lett. 65 (1990) 3100
[12] D.E. DiGregorio, K.T. Lesko, B.A. Harmon, J. Poulliot, B. Sur, Y. Chan and R.G. Stokstad, Phys. Rev. C42 (1990) 2108
[13] C.C. Sahm, H.-G. Clerc, K.-H. Schmidt, W. Reisdorf, P. Armbruster, F.P. Hessberger, J.G. Keller, G. Münzenberg and D. Vermeulen, Nucl. Phys. A441 (1985) 316
[14] F. Scarlassara, Proc. Symp. on heavy ion interactions around the Coulomb barrier, Legnaro, Italy, 1988, eds. C. Signorini, S. Skorka, P. Spolaore and A. Vitturi (Springer, Berlin, 1988) p. 79